Decay and Recurrences of Wave Packets in Nonlinear Quantum Systems[†]

A. A. Stuchebrukhov and R. A. Marcus*

Arthur Amos Noyes Laboratory of Chemical Physics, 127-72, California Institute of Technology, Pasadena, California 91125

Received: August 31, 1993; In Final Form: October 27, 1993®

A simple and analytical model of quantum recurrences in wave packet dynamics of nonlinear vibrational systems is presented. It is shown that in addition to "normal" rephasing time τ_R the width of the packet experiences very strong recurrences at $\tau_R/2$. In a quasiclassical limit, which can be studied explicitly in this model, the recurrences disappear and the decay becomes irreversible. Recent femtosecond experimental results of Zewail and co-workers are discussed in the framework of this analytical model.

1. Introduction

In general, quantum recurrences in dynamics of wave packets are associated with discreteness of the energy spectrum (perhaps with some broadening, and which is observed as a structure in the absorption spectrum). One example of a system with recurrences discussed in the chemical physics literature is the famous Bixon-Jortner model, which describes decay of a single zero-order state into a manifold of equally spaced backgriound states. This model played an important role in understanding the nature of the irreversibility of radiationless transitions in isolated polyatomic molecules. The discreteness of the spectrum of the background states results in the recurrences in this model. Another example of recurrences has been found in the wave packet dynamics of molecular vibrations. Recurrences in this case are observed in time-resolved experiments as "quantum beats" of coherently excited quantum states.

Recently Zewail and co-workers¹⁰⁻¹⁴ observed the decay and recurrences of initially prepared localized wave packets of nuclear coordinates of diatomic molecules. NaI and other diatomic molecules were studied in the femtosecond time-resolved experiments. In these experiments the decay signal was measured in real time for the dissociated molecules. The latter contribute to the signal as the wave packet sweeps through the region of crossing of stable and unstable potential curves. Chapman and Child¹⁵ calculated lifetimes of the predissociating states in NaI and discussed the observed recurrence phenomena using a numerical simulation of the wave packet dynamics. The wave packet dynamics has also been studied in numerical simulations by other researchers, e.g., as in refs 16 and 17.

In addition to the expected long-time recurrence with a period inversely proportional to the local anharmonicity, an unusual recurrence at half of the period of this expected recurrence occurred in the experiments¹³ as well as in the numerical simulations. The purpose of this paper is to present an analytical model which allows one to obtain additional insight into the nature of this phenomenon.

We consider the evolution of an initially prepared coherent state¹⁸ (a Gaussian wave packet in coordinate space) in an anharmonic vibrational mode and study the dynamics of the center of mass of the packet and its width. The approach is an extension of that used in a recent paper,¹⁹ where the angle-action representation for the semiclassical wave packet dynamics was used. The anharmonicity of the mode causes a spread of the wave packet, and the quantum nature of the system, i.e., discreteness of the spectrum, results in recurrences. We will show that the classical limit of this model corresponds to the continuous approximation of a discrete (quantum) action variable

and to an approximate calculation of certain sums, by replacing them with integrals over the continuous action variable. This procedure is equivalent to a continuum approximation of the energy spectrum of the system. The present model allows one to trace what happens to the recurrences in this approximation. We also calculate and discuss, in the framework of this model, the form of the time-domain signal describing the dissociating molecules as the wave packet sweeps back and forth through the tunneling region in coordinate space.

The structure of the paper is as follows. In sections 2 and 3 the Hamiltonian and the initial state are discussed. In sections 4 and 5 the analytical solutions for the dynamics of the center of mass and the width of the wave packet are described. The results are used then in section 6 to discuss comparison with the experimental data on the femtosecond predissociation of NaI. It is shown in this section that our analytical solution displays a feature in the wavepacket dynamics similar to that reported in the experiment. In section 7 the continuum approximation is discussed which provides an additional insight into the nature of the recurrences.

2. Hamiltonian, Complex Phase Space, and Averages

We consider a nonlinear vibrational mode with the Hamiltonian of the form $(\hbar = 1)$

$$\hat{H} = \omega_0 \left(\hat{n} + \frac{1}{2} \right) - \chi \omega_0 \left(\hat{n} + \frac{1}{2} \right)^2 \tag{2.1}$$

where \hat{n} is the occupation number operator, $\hat{n} = \hat{a}^{\dagger}\hat{a}$, and \hat{a} , \hat{a}^{\dagger} are annihilation and creation operators, so that

$$\hat{n} = \frac{\hat{x}^2 + \hat{p}^2}{2} \tag{2.2}$$

with x and p being the dimensionless coordinate and the canonically conjugate momentum respectively. (The usual units are recovered by substitution $x \to x(m\omega_0/\hbar)^{1/2}$ and $p \to p(m/\hbar\omega_0)^{1/2}$, where m is the mass.) This Hamiltonian yields the energy spectrum

$$E_n = \omega_0 \left(n + \frac{1}{2} \right) - \chi \omega_0 \left(n + \frac{1}{2} \right)^2 \tag{2.3}$$

For a positive χ , eqs 2.1-2.3 describe a second-order perturbation vibrational Hamiltonian, when x and p are conventional coordinate and momentum. If, instead, the H in (2.1) referred to a Morse-type spectrum, the x and p in (2.2) would no longer be the conventional coordinate and momentum exactly. In this case, however, they still may provide the Cartesian coordinate and momentum in a zeroth-order anharmonic approximation. The quality of this approximation depends of the anharmonicity parameter χ . This approximation is not, however, restricted to

[†] Contribution No. 8856.

Abstract published in Advance ACS Abstracts, March 1, 1994.

nearly harmonic potential surfaces. As long as the local energy spectrum is smooth and can be presented as a quadratic approximation in action space, as in eq 2.3, then our approximation is accurate. In this case, the local frequency, ω_0 , is itself a smooth function of energy.

The wave packet is described by a state $|\psi(t)\rangle$, which evolves in time from the initially prepared state $|\psi(0)\rangle$. We are interested in the evolution of two observables, one describing the center of mass of the packet and the other its width:

$$x(t) \equiv \langle x(t) \rangle = \langle \psi(t) | x | \psi(t) \rangle = \langle \psi(0) | x(t) | \psi(0) \rangle \quad (2.4)$$

$$\sigma^{2}(t) = \bar{x}^{2}(t) - \bar{x}^{2}(t) \tag{2.5}$$

where we will use either a bar or () to denote an average over the packet. The meaning of $\sigma^2(t)$ will be seen most clearly in eq 6.1 later. Because of the relations $\hat{a} = (\hat{x} + i\hat{p})/\sqrt{2}$ and $\hat{a}^{\dagger} =$ $(\hat{x}-i\hat{p})/\sqrt{2}$, one can find $\langle a(t)\rangle$ and $\langle a^{\dagger}(t)\rangle$ instead of $\langle x(t)\rangle$, and $\langle a^2(t) \rangle$ and $\langle a^2 \uparrow(t) \rangle$ instead of $\langle x^2(t) \rangle$, in order to calculate $\langle x(t) \rangle$ and $\sigma^2(t)$. The operators $\hat{a}(t)$ and $\hat{a}^{\dagger}(t)$ describe the evolution of the system in the complex phase space $(x \pm$ $ip)/\sqrt{2}$. For these operators the Heisenburg equations read

$$\mathrm{d}\hat{a}/\mathrm{d}t = -i(\omega_0 - 2\chi\omega_0(\hat{n} + 1))\hat{a} \tag{2.6a}$$

$$d\hat{a}^2/dt = -2i(\omega_0 - 2\chi\omega_0(\hat{n} + 3/2))\hat{a}^2 \qquad (2.6b)$$

Here, because $\hat{H} \equiv H(\hat{n})$, the occupation number operator, \hat{n} , is a constant of motion. This property allows one to write the solutions of the Heisenberg equations, (2.6), in an explicit operator form

$$\hat{a}(t) = \exp[-i(\omega_0 - 2\chi\omega_0(\hat{n} + 1))t]\hat{a}(0)$$
 (2.7a)

$$\hat{a}^{2}(t) = \exp[-2i(\omega_{0} - 2\chi\omega_{0}(\hat{n} + ^{3}/_{2}))t]\hat{a}^{2}(0) \quad (2.7b)$$

These solutions can be used to calculate the averages of present interest

$$\langle a(t)\rangle = \sum_{n} [g_n e^{-i(\omega_0 - 2\chi\omega_0(n+1))t}] \langle a(0)\rangle \qquad (2.8a)$$

$$\langle a^2(t) \rangle = \sum_{n} \left[d_n e^{-2i(\omega_0 - 2\chi\omega_0(n+3/2))t} \right] \langle a^2(0) \rangle \quad (2.8b)$$

where the weighting factors, g_n and d_n

$$g_n = c_n^* \langle n | a | \psi(0) \rangle / \langle a(0) \rangle \tag{2.9a}$$

$$d_n = c_n * \langle n | a^2 | \psi(0) \rangle / \langle a^2(0) \rangle$$
 (2.9b)

have been introduced. These quantities are expressed in terms of the amplitudes, c_n , of the expansion of the initial state of the system in tiers of the eigenstates of the Hamiltonian H, $|n\rangle$

$$|\psi(0)\rangle = \sum_{n} c_n |n\rangle \tag{2.10}$$

Equations 2.8 constitute the basis of the present model.

Using (2.4) and (2.5) the center of mass of the wave packet, $\bar{x}(t)$, and the width of the packet, $\sigma^2(t)$, are given by

$$\tilde{x}(t) = 2^{1/2} Re \langle a(t) \rangle \tag{2.11a}$$

$$\sigma^{2}(t) = (\bar{n} + \frac{1}{2}) + Re(\langle a^{2}(t) \rangle - \langle a(t) \rangle^{2}) - \langle a(t) \rangle \langle a^{\dagger}(t) \rangle$$
(2.11b)

where \bar{n} is the average value of n in the packet.

For a harmonic system, where $\chi = 0$, there is no decay of the wave packet and (2.8) gives, as one expects, $\langle a(t) \rangle \sim e^{-i\omega_0 t}$ and $\langle a^2(t)\rangle \sim e^{-2i\omega_0 t}$. When $\chi \neq 0$, a dephasing of oscillating exponentials in (2.8) occurs, resulting in a decay of the initial

packet. However, due to the discreteness of the frequencies of the oscillating exponentials, there will be also recurrences, as a result of rephasing. These recurrences are considered below in this paper.

3. Initial State: Coherent and Squeezed States

Short optical femtosecond pulses have been used in some recent experiments on real-time dynamics in molecular systems. When the spectral width of the laser pulse is much larger than the absorption envelope, the Franck-Condon principle applies and the probability distribution of vibrational states in the wave packet formed on the upper electronic state is approximately Gaussian. (In the opposite case, when the pulse length is longer than the inverse band width of the absorption spectrum, only a prtion of the energy spectrum of the Franck-Condon envelop will be produced. The latter situation is closer than the former one to the case of the NaI system studied experimentally. 10-14 Thus our comparison with experimental observations, discussed later in the paper, is of qualitative character.) This distribution in the coordinate space is close to that in the initial, i.e., the ground vibrational state of the molecule. Under certain conditions, noted below, the initial state, $|\psi(0)\rangle$, on the upper electronic state can be described approximately by a coherent state 18,20

$$|\psi(0)\rangle = |\alpha\rangle = e^{-|\alpha|^2/2} \sum_{n} \frac{\alpha^n}{(n!)^{1/2}} |n\rangle$$
 (3.1)

where a complex value α is defined by the average initial value of the coordinate and conjugate momentum of the wave packet

$$\alpha = \frac{\bar{x} + i\bar{p}}{2^{1/2}} \tag{3.2}$$

where \bar{x} and \bar{p} denote averages for the initial wave packet.

If in the upper electronic state the equilibrium interatomic distance differs by δ from that in the lower electronic state, and the vibrational frequency in the upper state is the same as in the ground state, the initial state will be a "shifted" ground vibrational state, i.e., a coherent state. In such a state the shift $\bar{x} = \delta$ and the uncertainty of distribution of coordinate and momentum will be the minimum possible, i.e., $\Delta x \Delta p = 1/2$, and, moreover, Δx = $\Delta p = 1/2^{1/2}$. The average momentum remains unchanged, due to the Franck-Condon principle, $\bar{p} = 0$, thus in eqs 3.1 and $3.2 \alpha = \bar{x} = \delta$.

It should be noted that eq 3.1 describes the initial state in the upper electronic state exactly, after a short pulse excitation from the ground electronic state, only when the ground electronic state is harmonic and the vertically excited electronic state has the same local frequency (ω_0 in eq 2.1) as the ground state frequency.

In a more accurate description the vibrational frequency of the upper electronic state, ω_0^u , is different (smaller) from that in the lower state, ω_0^g . The consequence of such an "instantaneous" change of the vibrational frequency, in addition to the shift of the origin of the coordinates by δ , is that instead of a coherent state, with a symmetric distribution of x and p, $\Delta x = \Delta p = 1/2^{1/2}$, the initial vibrational state after the electronic excitation will be a so-called squeezed state. 21,22 In such a state the width of distribution of coordinates is smaller than that in the ground vibrational state (!) of the upper electronic state. (The distribution, however, remains the same as in the ground vibrational state of the lower electronic state.) This effect occurs because the (dimensionless) width of the coordinate distribution is proportional to $\kappa = (\omega_0^u/\omega_0^g)^{1/2}$. The momentum, on the other hand, is proportional to $1/\kappa$, and thus the joint distribution $\Delta x \Delta p$ remains the same, i.e., it has the minimum possible value 1/2. The dynamical consequence of such an asymmetry in the distribution of coordinates and momenta is that in the harmonic approximation

the wave packet width will oscillate with double the vibrational frequency ω_0^u . This result is easy to understand in the plane of dimensionless x and p, where all phase space points will move along the circles with the same angular frequency ω_0^u . Projection of any asymmetric distribution will periodically change its width twice during the vibrational period. In this paper we are interested in a much longer time scale evolution. Thus, we ignore such additional fast oscillations and, hence, neglect here the asymmetry between coordinate and momentum in the initial state. A more detailed description will be presented in a future publication.²³ Hence, our model provides only qualitatively correct description of the initial wave packet in the excited electronic state.

Different zeroth-order quantum states are populated in the initial wave packet (3.1) according to the Poisson distribution

$$p_n = |\langle n|a\rangle|^2 = e^{-|\alpha|^2 \frac{|\alpha|^{2n}}{n!}}$$
(3.3)

with an average $\bar{n} = |\alpha|^2$, as seen from eq 2.2. The width of the distribution in *n*-space is $(\bar{n})^{1/2}$ and in the vicinity of the maximum the distribution has the Gaussian form

$$p_n \simeq \frac{1}{(2\pi \bar{n})^{1/2}} \exp\left[-\frac{(n-\bar{n})^2}{2\bar{n}}\right]$$
 (3.4)

The coherent state (3.1) is also a Gaussian in the coordinate x-space.

The most important feature of the coherent state that we use is that $a|\alpha\rangle = \alpha|\alpha\rangle$. The usefulness of this equality is evident from (2.9). For a coherent state the distributions characterizing $\langle a(0) \rangle$ and $\langle a^2(0) \rangle$ for g_n and d_n in eq 2.9 take the form

$$g_n = d_n = p_n \tag{3.5}$$

I.e., they coincide with the distribution p_n in the initial state, given by eq 3.3. Another simplification of the calculation is that for a coherent state we have

$$\langle a(0) \rangle = \alpha \tag{3.6a}$$

$$\langle a^2(0) \rangle = \alpha^2 \tag{3.6b}$$

After the above explicit expressions for g_n and d_n are substituted from (3.5) and (3.3) and with use of (3.6), the time-evolution of averaged operators of present interest, (2.8), takes the form

$$\langle a(t) \rangle = \alpha e^{-\hbar(1-\cos(2\chi\omega_0 t))} e^{-i[(\omega_0 - \chi\omega_0)t - \hbar\sin(2\chi\omega_0 t)]}$$
 (3.7a)

$$\langle a^2(t) \rangle = \alpha^2 e^{-\hbar(1-\cos(4\chi\omega_0 t))} e^{-i[2(\omega_0 - 2\chi\omega_0)t - \hbar\sin(4\chi\omega_0 t)]}$$
 (3.7b)

These two formulas provide the solution to the problem of the time-evolution of the initial coherent state explicitly and allow a detailed analysis of the dynamics.

4. Dynamics of the Center of Mass of the Wave Packet

In the analysis we consider first eq 3.7a. The operator a(t) is a linear combination of coordinate and momentum operators, so that the average $\langle a(t) \rangle$ gives the position of the center of the wave packet in the complex plane

$$\langle a(t)\rangle = \frac{\bar{x}(t) + i\bar{p}(t)}{2^{1/2}} \tag{4.1}$$

For simplicity one can imagine that initially the center of the packet in the complex (x, p) plane is located at $\langle p(0) \rangle = 0$, in correspondence with the usual vibrational condition in the upper electronic state just after the excitation. In this case, using (3.2), $\alpha = \langle x(0) \rangle / 2^{1/2}$, where $\langle x(0) \rangle$ is the initial value of the center of mass coordinate of the wave packet.

The second exponential factor in (3.7a), which can be written as $\exp(-\phi(t))$, describes a rotation, $\phi(t)$, with a modulated

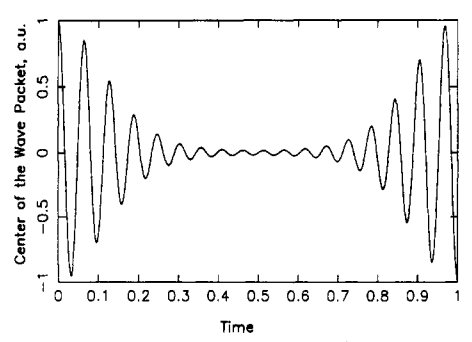


Figure 1. Time evolution of the center of mass of the wave packet. Initial state is a coherent state. Units for time is π/χ . Parameters: $\hbar = 3$, χ/ω_0

frequency, of the complex valued quantity $\langle a(t) \rangle$. The xcoordinate of $\langle a(t) \rangle$, i.e., the real part of it, gives the evolution of the center of the packet in real coordinate space, x. The phase in this factor can be written in terms of a time-dependent frequency $\omega(t)$, as $\int \omega(t) dt$, where

$$\omega(t) = \omega_0 - \chi \omega_0 + 2\chi \omega_0 \bar{n} \cos(2\chi \omega_0 t) \tag{4.2}$$

The modulated frequency oscillates in the interval $\omega_0 - \chi \omega_0 \pm$ $2\chi\omega_0\bar{n}$, and the frequency of modulations is $2\chi\omega_0$. The amplitude of modulations, $2\bar{n}\chi\omega_0$, is seen to depend upon the width of the

The first exponential factor in eq 3.7a, a real quantity, describes a variation of the absolute value of the $|\langle a(t)\rangle|$, which represents the distance of the center of mass of the packet from the center of coordinates, x = p = 0, in the complex plane. This variation has the same modulation frequency, $2\chi\omega_0$. The evolution of the center of mass of the packet is shown in Figure 1. In the case of a harmonic mode the center of the packet would move along a circle of a constant radius in the complex plane x + ip. For a nonlinear mode the center of the packet moves along a spiral toward the center of the coordinate system, reaches the center at $\tau_R/2 = \pi/2\chi\omega_0$, and then moves out along the same spiral, completing the recurrence at $\tau_R = \pi/\chi \omega_0$. The pulsating behavior of the center of the packet presents the first type of the recurrence which we discuss here. (The analogous behavior of the width of the packet presents the second type.)

5. Dynamics of the Width of the Wave Packet

We consider next the dynamics of the width of the wave packet. (2.5), which occurs coherently with the motion of the center of the wave packet described above and whose experimental study prompted the present paper.

Before we discuss the quantitative results for the present model, it is useful to discuss the qualitative picture in harmonic and anharmonic cases.²⁴ In a harmonic case, for any initial wave packet, $\langle x(t) \rangle$ has a pure harmonic $\exp(i\omega_0 t)$ time dependence due to the harmonic oscillator selection rule that only states differing by ±1 quanta have nonzero matrix elements. Removing this restriction in the anharmonic case gives higher harmonics to $\langle x(t) \rangle$, but the latter is still periodic with period $2\pi/\omega_0$. A general wave packet in a harmonic potential has a width that has a time dependence of a constant plus a term that oscillates with an angular frequency $2\omega_0$; that is the wave packet expands and then contracts to its initial value at a time of half the classical oscillation period. The reason is due to the harmonic selection rule. The width depends upon $\langle x^2(t) \rangle - \langle x(t) \rangle^2$. The x^2 operator has matrix elements that are diagonal (which leads to the time-independent contribution to the width) and off-diagonal by ± 2 , which gives a pure harmonic $\exp(2i\omega_0 t)$ time dependence.

When the anharmonic case is considered (but with harmonic matrix elements, as assumed in the present paper), the various terms in $\langle x(t) \rangle$ no longer oscillate at the same frequency, but at frequencies that differ by multiples of $2\chi\omega_0$. These terms will

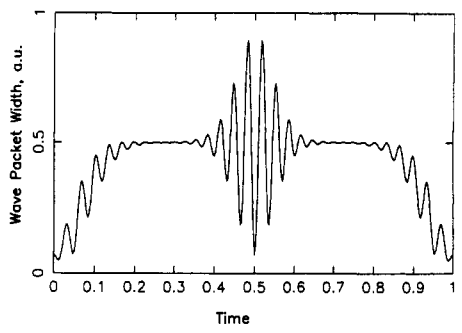


Figure 2. Time evolution of the wave packet width. The units and parameters are the same as in Figure 1.

all rephase at $\tau_R = \pi/\chi\omega_0$. Similarly, the terms contributing to the oscillations in the variance of the wave packet differ in frequency by multiples of $4\chi\omega_0$, and these cause the width to dephase and then rephase at a time $\pi/2\chi\omega_0 = \tau_R/2$ (the dephasing time is just $\tau_R/\Delta n$, where Δn is the width of the wave packet in quantum numbers). Thus, we expect this picture to hold for a fairly general anharmonic case and to be independent of the initial shape of the wave packet. We proceed next with more accurate calculations of our model.

The analysis of (3.7b), similar to that of (3.7a), gives an explicit expression for the width in coordinate space

$$\sigma^{2}(t) = \frac{1}{2} + \bar{n}(1 - e^{-2\bar{n}(1 - \cos(2\chi\omega_{0}t))}) + \\ \bar{n}e^{-2\bar{n}(1 - \cos(2\chi\omega_{0}t))}\cos(2(\omega_{0} - \chi\omega_{0})t - 2\bar{n}\sin(2\chi\omega_{0}t)) - \\ \bar{n}e^{-\bar{n}(1 - \cos(4\chi\omega_{0}t))}\cos(2(\omega_{0} - 2\chi\omega_{0})t - \bar{n}\sin(4\chi\omega_{0}t))$$
(5.1)

This expression contains two time scales defined by ω_0 and $\chi\omega_0$. We first suppose that these two time scales are well separated. To simplify the dynamics, we first average the whole expression over the fast period $2\pi/\omega_0$, which leaves a simplified expression for the width

$$\sigma^{2}(t) = \frac{1}{2} + \bar{n}(1 - e^{-2\hbar(1 - \cos(2\chi\omega_{0}t))})$$
 (5.2)

Initially the width of the packet is seen to be 1/2, which corresponds to minimum uncertainty in the coherent state. 18,20 There is then an increase of the width, due to dephasing, as the center of the packet approaches the center of coordinates in the phase space (x, p). The rate of the broadening of the wave packet is defined by the classical spread of the frequencies in the packet. If the spread of the frequencies is relatively large and if anharmonic constant is small, the center of the packet will spend much of the time in the vicinity of the poing (x,p) = (0,0), while the width of the packet will be very close to a microcanonical average value $\bar{n} + 1/2$. This type of the behavior resembles relaxation to some average microcanonical equilibrium. However, when time approaches $\tau_R = \pi/\chi\omega_0$, the wave packet shrinks back to the initial width 1/2 due to rephasing. This purely quantum effect is absent in the continuum (classical) picture described below in section 7. The latter can be obtained, as will be seen below, by a formal expansion in the small constant $\chi\omega_0$. The first terms of the expansion result in a decay of the wave packet to a microcanonicallike distribution with the width $\sigma^2 = 1/2 + \bar{n}$. (We note that in the usual units of length, the width is $(1/2 + \bar{n})\hbar/m\omega_0$. In the semiclassical limit when $h \rightarrow 0$, an initial width of the wave packet $\hbar/2m\omega_0 \rightarrow 0$. However, the width grows at later times to a microcanonical value $\hbar \bar{n}/m\omega_0$, due to the spread of frequencies in the wave packet. Because \bar{n} is proportional to \hbar^{-1} at finite action, the microcanonical width is finite as $\hbar \rightarrow 0$).

A complete recurrence at $\tau_R = \pi/\chi\omega_0$ is not the only quantum effect. We consider now an exact wave packet dynamics with the fast oscillations included, as in (5.1). The typical evolution is shown in Figure 2. The most interesting feature here is the fast and very large oscillations of the width when the center of the

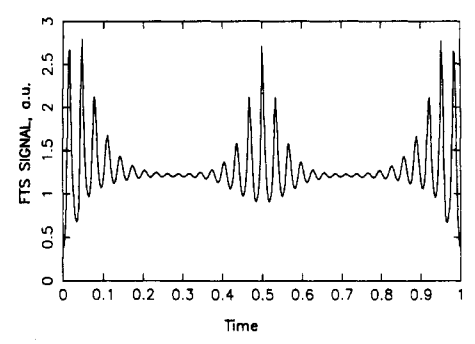


Figure 3. Theoretical FTS signal corresponding to a modulated part of the experimental signal of ref 13. (FTS stands for femtosecond transitionstate spectroscopy. 10-14)

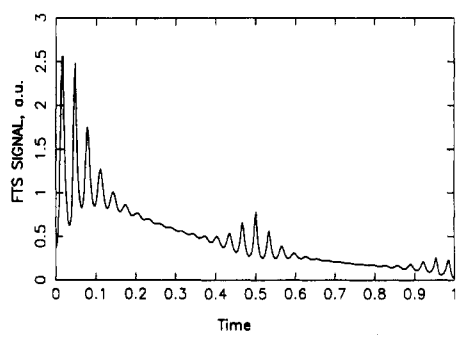


Figure 4. Theoretical FTS signal with a single-exponential decay rate. packet is in the vicinity of the zero point. These oscillations take place at exactly half the period of the normal recurrence time, $\tau_R/2 = (\pi/\chi\omega_0)/2$. Again, these oscillations are absent in the continuum picture. The nature of this type of recurrences, as in the case with $\langle a(t) \rangle$, is connected with stepwise nature of vibrational amplitudes mixed in the wave packet. It is interesting to note that this type of recurrence, with a half-period of the usual recurrence time, may be the factor responsible for the observed features in the decay signal in ref 13, which we discuss below.

6. Dynamics of the Probability Denisty. Experimental Signal

We can make use of the analytical formulas 3.7a and 5.1 to calculate the time evolution of the probability density of the wave packet at some fixed point in the coordinate space. This value is proportional to the experimental signal of both the laser-induced fluorescence and, in the case of vibrational predissociation, of dissociating molecules due to "leaking" through the region of intersection of stable and unstable potential curves.¹³ For the latter case we do not take into account the decrease of population in the packet due to dissociation and any difference in dissociation rate from different quantum states.15

The density can be calculated by the Gaussian approximation for the packet

$$\rho(x) = (2\pi\sigma^2(t))^{-1/2} \exp(-(x - \bar{x}(t))^2 / 2\sigma^2(t))$$
 (6.1)

where $\bar{x}(t)$ is the real part of (3.7a) and $\sigma^2(t)$ is that of (5.1). The time evolution predicted by this formula at x = 0 is shown in Figure 3. We note a feature of the signal at half-period of the normal recurrence time, $\tau_R/2 = \pi/2\chi\omega_0$. The simulated exponential depletion of the total population in the packet due to dissociation is shown in Figure 4. Both results, Figures 3 and 4, are in a qualitative agreement with the experimental decay signal of ref 13, where the authors reported a pronounced tendency for the signal from NaI to recur both at normal recurrence time (about 30 ps) and exactly half the the normal recurrence time (about 15 ps).

7. Continuum Limit

To understand better the origin of the recurrences discussed

above in the present paper, it is useful to compare the above result with that which is obtained in the limit when $\bar{n} \gg 1$ and when the variable n is treated as a continuous variable, as in the classical case. In this case for a constant classical action of the oscillator $J = 2\pi \hbar n$, n is proportional to \hbar^{-1} . At the same time in order to have a finite anharmonic shift, as for example in eq 7.2 below, χ must be proportional to \hbar . Hence, χ vanishes as $\hbar \to 0$. However, the product $n\chi$ remains finite in the classical limit.

For simplicity we consider only the behavior of the center of mass of the packet.

For the distribution function we can now substitute (3.4) instead of (3.3). Replacing the summation in (2.8a) by an integration over n (and noting that substitution (3.4) is equivalent to the integration by the steepest descent method) yields the result

$$\langle a(t) \rangle_{\text{scl}} = \alpha e^{-2\chi^2 \omega_0^2 \hbar t^2} e^{-i(\omega_0 - 2\chi \omega_0(\hbar^{+1}/2))t}$$
 (7.1)

Comparison of this expression with quantum formula 3.7a reveals several interesting features.

First, there is no longer a modulation of the frequency of rotation of the wave packet around the center of coordinates in the complex plane (x,p). The rotation frequency now coincides with the classical anharmonic local frequency of vibrations which depends, in turn, on the classical amplitude of the vibration. This local frequency is an average

$$\langle \omega_{n,n+1} \rangle = \langle E_{n+1} - E_n \rangle = \omega_0 - 2\chi \omega_0(\bar{n} + \frac{1}{2}) \quad (7.2)$$

It is seen from this expression that for the limit of large n to be explored at a meaningful, i.e., finite, anharmonic frequency, the $2\chi\omega_0n$ must remain finite as $\bar{n}\to\infty$. Hence, $\chi\omega_0$ must tend to zero, thus explaining how (7.1) immediately follows from (3.7a). (Alternatively, had we not used units of $\hbar = 1$, we would have $\chi\omega\sim\hbar\rightarrow0$; however $\chi\omega_0\bar{n}$ would remain finite, as we noted above.)

Second, a pure real exponential factor in eq 7.1 now describes a trivial decay of the amplitude of vibrations of the wave packet. This decay is a a consequence of dephasing of the oscillating exponentials with different frequencies mixed in the wave packet. The vibrational frequencies depend on the amplitude of vibrations, $\omega(n) = \omega_0 - 2\chi \omega_0 (n + 1/2)$, and, hence, the spread of the frequencies is defined, in the classical language, by the spread of the amplitudes of vibrations, $\langle (n-\bar{n})^2 \rangle = \bar{n}$, according to (3.3). The spread of frequencies then equals $2\chi^2\omega_0^2\bar{n}$, in correspondence with the decay rate of (7.1). In this limit, described by eq 7.1, the center of the wave packet approaches asymptotically the center of the coordinate system, x = 0, p = 0. This behavior does not mean, of course, that the energy is not conserved. As is shown in section 5, this process is accompanied by the spread of the wave packet. (We note that in the true classical limit, however, when h = 0, the width of the initial packet, which is described in the present paper by a coherent state (3.1), is zero. In this limit, the semiclassical dephasing described by the first exponential in eq 7.1 is absent, simply because the decay time, proportional to $\hbar^{-1/2}$, becomes infinitely large.)

Thus, in contrast to the full quantum case, the the center of the wave packet in the above approximation approaches the zero point of the coordinate system asymptotically and never returns to the initial position. The recurrences observed in the quantum case are the consequence of a quantization of the amplitudes (or energies) of vibrations in (2.8). This quantization makes the dynamics of the wave packet quasiperiodic. The quantum nature of the final result (3.7) reveals itself in that the anharmonic constant, $\chi\omega_0$, enters the equation by itself, rather than being multiplied by the large classical square amplitude, ħ. Really, the anharmonic constant gives the increase (or decrease) of the frequency of vibrations when the square of the amplitude of vibrations is changed in our units by 1. In the continuum approximation (7.1), where the square amplitude of the vibration $n \gg 1$, such change is insignificant. Hence, the small frequency

 $\chi\omega_0$ should be regarded formally as vanishingly small. This idea can be confirmed by taking the limit $\chi \omega_0 \sim \hbar \rightarrow 0$ of the quantum expression (3.7). The first nonvanishing terms give the continuum result (7.1). The period of the quantum recurrences due to anharmonicity, $\pi/\chi\omega_0$, becomes infinitely large in the continuum limit, when $\chi\omega_0 \rightarrow 0$. This behavior is analogous to that of the recurrence period of the Bixon-Jortner model; namely, when the spacing between adjacent levels of the background manifold, Δ , of that model diminishes to zero, the recurrence period becomes infinitely large.^{1,5} The anharmonic constant $\chi\omega_0$ in the present model describes spacings of the adjacent frequencies $(\omega_{n+1} - \omega_n)$ of the anharmonic oscillator and plays a role analogous to the spacings of the energy levels Δ of the Bixon-Jortner model.

8. Conclusion

In this paper we have presented a simple and exactly solvable analytic model which explains the main quantum effects of recurrences in the dynamics of a wave packet in an anharmonic vibrational system. The advantage of this model is that the nature of quantum recurrence effects can be studied analytically. We have shown, in particular, that the width of the initially prepared coherent state, after relaxation to a microcanonical-like equilibrium, experiences strong recurrences at a half-time of the total recurrence time. The analytical solution obtained in the present paper provides the insight into the nature of recurrences at a half-time of the normal recurrence time.

Acknowledgment. It is a great pleasure to dedicate this paper to our friend and colleague, Joshua Jortner, on the occasion of his sixtieth birthday. We would like to acknowledge the discussion of results of this paper with Kevin Lehmann and Ahmed Zewail. The financial support of the National Science Foundation is also greatly acknowledged. This work is part of the Caltech-JPL Supercomputing Project Collaboration.

References and Notes

- (1) Bixon, M.; Jortner, J. J. Chem. Phys. 1968, 48, 715.
- (2) Freed, K. In Radiationless Processes in Molecules and Condensed Phases; F. K. Fong, F. K., Ed.; Springer: New York, 1976; Vol. 15, pp 23-
 - (3) Freed, K. Top. Curr. Chem. 1972, 31, 105.
 - (4) Freed, K. J. Chem. Phys. 1970, 52, 1345.
- (5) Medvedev, E. S.; Ohserov, V. I. Theory of Radiationless Transitions in Polyatomic Molecules; Springer: New York, 1991.
- (6) Heller, E. J. Wavepacket Dynamics and Quantum Chaology. In Chaos and Quantum Physics; NATO Les Houches Lecture Notes; North-Holland: Amsterdam, 1990.
 - (7) Uzer, T. Phys. Rep. 1990, 199, 75.
- (8) Chirikov, B. V.; Izrailev, F. M.; Shepelansky, D. L. Sov. Sci. Rev. 1982, 2C, 209.
 - (9) Zaslavsky, G. M. Phys. Rep. 1981, 80, 157.
- (10) Gruebele, M.; Zewail, A. Phys. Today 1990, 43, (No. 5), 24. (11) Gruebele, M.; Roberts, G.; Dantus, M.; Bowman, R. M.; Zewail, A.
- H. Chem. Phys. Lett. 1990, 166, 459.
- (12) Gerdy, J. J.; Dantus, M.; Bowman, R. M.; Zewail, A. H. Chem. Phys. Lett. 1990, 171, 1. (13) Cong, P.; Mokhtari, A.; Zewail, A. H. Chem. Phys. Lett. 1990, 172, 109.
- (14) Rose, T. S.; Rosker, M.; Zewail, A. H. Chem. Phys. Lett. 1989, 91, 7415.
 - (15) Chapman, S.; Child, M. S. J. Phys. Chem. 1991, 95, 578.
 (16) Choi, S.; Light, J. C. J. Chem. Phys. 1989, 90, 2593.
 (17) Engel, V.; Metiu, H. J. Chem. Phys. 1989, 90, 6116.
- (18) Cohen-Tannoudji, C.; Diu, B.; Laloe, F. Quantum Mechanics; Wiley: New York, 1977
- (19) Marcus, R. A. Chem. Phys. Lett. 1988, 152, 8.
- (20) Klauder, J. R.; Sudarshan, I. C. Fundamentals of Quantum Optics; Benjamin: New York, Amsterdam, 1868.

 - (21) Walls, D. F. Nature (London) 1983, 306, 141.
 (22) Squeezed Light. Special Issue, J. Mod. Optics 1987, 34, 709-1020.
 (23) Stuchebrukhov, A. A.; Marcus, R. A. To be submitted.
- (24) We are indebted to Professor Kevin Lehmann for this qualitative insight.